HHS Public Access

Author manuscript

J Toxicol Environ Health A. Author manuscript; available in PMC 2023 June 03.

Published in final edited form as:

J Toxicol Environ Health A. 2022 June 03; 85(11): 439–456. doi:10.1080/15287394.2022.2032518.

Effects of life-stage and passive tobacco smoke exposure on pulmonary innate immunity and influenza infection in mice

Lei Wang[1,*], **Maya Rajavel**[1,*], **Ching-Wen Wu**[1,*], **Chuanzhen Zhang**[1,2], **Morgan Poindexter**[1], **Ciara Fulgar**[1], **Tiffany Mar**[1], **Jasmine Singh**[1], **Jaspreet K. Dhillon**[1], **Jingjing Zhang**[1,3], **Yinyu Yuan**[1], **Radek Abarca**[1], **Wei Li**[4], **Kent E. Pinkerton**[1,5]

[1]Center for Health and the Environment, University of California, Davis, CA, USA

[2]Department of Gastroenterology, the First Affiliated Hospital of Shandong First Medical University, Shandong Provincial Qianfoshan Hospital, Jinan, Shandong 250014, China

[3]Western China School of Public Health Department of Occupational and Environmental Health Sichuan University, Chengdu, China

[4]School of Control Science and Engineering, Shandong University, Jinan, Shandong 250014, China

[5]Department of Pediatrics, University of California, Davis, CA, USA

Abstract

Limited data are available on the effects of perinatal environmental tobacco smoke (ETS) exposure for early childhood influenza infection. The aim of the present study was to examine whether perinatal versus adult ETS exposure might provoke more severe systemic and pulmonary innate immune responses in influenza A/Puerto Rico/8/34 virus (IAV)-inoculated compared to phosphate-buffered saline (PBS) mice. BALB/c mice were exposed to filtered air (FA) or ETS for 6 weeks during the perinatal or adult period of life. Immediately following final exposure, mice were intranasally inoculated with IAV) or PBS. Significant inflammatory effects were observed in bronchoalveolar lavage fluid of neonates inoculated with IAV (FA+IAV or ETS+IAV) compared to ETS+PBS or FA+PBS, and in the lung parenchyma of neonates administered ETS+IAV versus FA+IAV. Type I and III interferons were also elevated in the spleens of neonates, but not adults with ETS+IAV versus FA+IAV exposure. Both IAV-inoculated neonate groups exhibited significantly elevated more CD4 T cells and increasing number of CD8 and CD25 T cells in lungs relative to adults. Taken together, these results suggest perinatal ETS exposure induces an exaggerated innate immune response which may overwhelm protective anti-inflammatory defenses against IAV and enhances severity of infection in infants and young children.

Correspondence: Kent E. Pinkerton, Ph.D., Center for Health and the Environment, University of California, Davis, Davis, CA 95616, TEL: (530) 752-8334, kepinkerton@ucdavis.edu.

*These authors contributed equally to this research.

DISCLOSURE STATEMENT

The authors declare that there is no conflict of interest.

Keywords

Environmental tobacco smoke; lung; immune response; influenza virus

INTRODUCTION

Tobacco use in the United States (U.S.) has decreased since 1965, but smoking still remains a habit for a large portion of the U.S. population (CDC 2014). Cigarette smoke contains approximately 5,000 chemicals including known human carcinogens (Nooshinfar et al. 2017), which, when inhaled, produces adverse lung health outcomes such as chronic obstructive pulmonary disease (COPD), emphysema, lung cancer, and heart disease (Lee et al. 2018). Adverse pulmonary outcomes are not limited to smokers, but extend to individuals passively exposed to tobacco smoke. Passive such as second- or third-hand tobacco smoke exposures are also known as environmental tobacco smoke (ETS) exposures. In addition to initiating the aforementioned diseases in adults, ETS exposure was reported to 1) produce adverse effects such as asthma attacks and respiratory infections in infants and children (CDC 2014); 2) worsen conditions of pre-existing diseases; and 3) result in death of at least 600,000 non-smokers annually (Han et al. 2011; Torres et al. 2012; Pacheco et al. 2013). However, less is known regarding the direct impact of ETS on pulmonary immune system, especially in children as compared to adults.

In the U.S., approximately 40% of children of the age 3 to 11 years are exposed to second-hand smoke (CDC 2020). Second-hand smoke or ETS exposure has been associated with reduced physiological lung function, higher frequencies of self-reported respiratory infections, and adverse respiratory symptoms in school-aged children (Fernández-Plata et al. 2016). ETS exposure was also shown to be a significant risk factor for reduced lung function and respiratory disease in young adults (Holmes and Ling 2017). Children can be highly susceptible to infection due to immature immune defenses and respiratory systems. Each year, more than 200,000 individuals are hospitalized for respiratory and heart condition illnesses attributed to influenza viral infection in the U.S. (Thompson et al. 2009). Approximately 50,000 children younger than 5 years are hospitalized due to seasonal influenza-related complications (Thompson et al. 2004). In the U.S., during the 2018–2019 flu season, 33 of 50 states reported the highest levels of influenza infection compared to previous years (Xu et al. 2019). Therefore, a study comparing the immune system impacts resulting from experimentally-controlled, concomitant exposures to ETS and influenza in neonates and adults is merited.

Previous investigators found enhanced inflammatory responses to viral infection in young mice with perinatal ETS exposure (Claude et al. 2012) or adult mice with short-term ETS exposure (Gualano et al. 2008). However, a comparison study between neonates and adults with controlled ETS exposure duration has not been done previously. To that end, the present study aimed to determine the effects of age, ETS exposure, and Influenza A/PR/8/34 virus (IAV)-inoculation on innate immune responses of mice. Neonatal exposure to environmental toxicants, such as ETS, were shown to adversely influence the function and maturation of human fetal tissues to impede pulmonary cell differentiation, metabolic

functions, and immune defenses, as well as enhance susceptibility to viral infections later in life (Hanson et al. 2012; Hollams et al. 2014). A number of studies demonstrated that neonatal development of the immune system is adversely impacted by ETS exposure during gestation and childhood (Yu et al. 2008; Cao et al. 2016). Given these past study findings, it was postulated that neonatal mice exposed to ETS in the present study might be more sensitive to IAV compared to their adult counterparts.

Infiltration of immune cells in bronchoalveolar lavage fluid (BALF), inflammation of lung tissue (histopathology), distribution of CD4-, CD8-, and CD25-positive T cell markers in lung tissue, and expression of interferon (*IFN*) mRNA in spleen tissue were determined following IAV inoculation. T cells are the most important lymphocyte trafficking to the lungs during the first week of viral infection. The CD4, CD8, and CD25 T cell markers were selected to visualize populations of helper, cytotoxic, and regulatory T cells, respectively. CD4-positive, helper, T cells interact with antigen-presenting cells (e.g., macrophages) to shape pathogen-specific, adaptive immune responses such as antibody production and cytotoxic T cell activation (Figure 1; Sant et al. 2018a; 2018b; Lee and Lawrence 2018). CD8-positive, cytotoxic, T cells induce death of pathogen-infected, damaged, or dysfunctional cells (Smed-Sörensen et al. 2012; Pizzolla et al. 2017). CD25-positive, regulatory T cells are a subset of CD4-positive cells which suppress the activities of other T cells, B cells, and antigen-presenting cells (Corthay 2009). These three cell types are important factors in the immune response to viral infections (Rosendahl Huber et al. 2014).

Interferons(IFNs) are recognized as an essential part of the innate and adaptive immune responses to viral infection [Figure 1; (Colonna et al 2002)]. IFNs are secreted by many cell types, with *IFN-α* produced by cells of the lymphoid lineage (e.g., T and B cells), *IFN-β* produced by epithelial and fibroblast cells, and *IFN-γ* (a key cytokine for innate and adaptive immunity targeting viral infection) produced by natural killer cells, CD8 T cells, B cells, macrophages, and dendritic cells (Kubota and Kadoya 2011). IFN-producing cells (IPCs) found in mouse spleen tissues produce type 1 IFNs (*IFN-α* and *β*) in response to physically and chemically inactivated virus (Miller and Anders 2003). *IFN-α* and *β* were reported to play an important role in promoting survival of activated lymphocytes, whereas *IFN-γ* contributes to activation and differentiation of lymphocytes and macrophages, as well as regulates the balance of cytokine production during immune responses (Price et al 2000).

A mouse model was used in the present study. Since mice are not natural hosts for influenza viruses, influenza test strains were adapted to more efficiently attach to alveolar and epithelial cells in bronchi, replicate, suppress immunity, and exhibit virulence in the mouse (Kamal et al 2014). The adaptation of the virus via engineered mutations makes the lung pathology of the mouse model similar to that of humans (Ilyushina et al. 2010). Murine-adapted strains influenza virus strains include influenza A/Puerto Rico/8/34, influenza A/WSN/33, and influenza B/Lee/1940 (Radigan et al. 2015). It was reported that with sufficiently large viral load inoculation, infection of BALB/c mice with the influenza A/Puerto Rico/8/34 viral strain results in severe pneumonia and increased mortality rates (Radigan et al. 2015). To study an animal model moderately infected by murine-adapted viruses might help to understand more comprehensively the biology of viral infection and host immune responses.

MATERIALS AND METHODS

Animal models

A total of 56 adult (6- to 8-week-old) BALB/c Swiss-Webster mice were purchased from Harlan Laboratories (Livermore, CA). These rodents included 32 timed-pregnant dams (gestational day (GD) 14), 12 males, and 12 non-pregnant females. The dams were time-mated with males by the vendor before shipment. Upon arrival, the dams were randomly assigned for filtered air (FA; control; n = 21) or ETS (n = 11) exposure to obtain neonatal groups exposed *in utero*. The male and non-pregnant female adult mice were randomly divided into 4 exposure groups with 6 adult mice (n = 3/gender) per group. The adult exposure groups were for FA+ phosphate-buffered saline (PBS), FA+IAV, ETS+PBS, and ETS+IAV.

The FA-exposed dams (n=21) birthed 69 pups, yielding a total of 22 male and 47 female pups, and ETS-exposed dams (n=11) birthed 68 pups, yielding a total of 27 male and 41 female pups. The FA-exposed individual pups from each litter were randomly assigned into the neonatal FA+ PBS (n = 10 male, 25 female) and FA+ IAV (n = 12 male and 22 female) groups, while individual pups from each ETS-exposed litters were also randomly assigned into the neonatal ETS+PBS (n = 12 male, 21 female) and ETS+IAV (n = 15 male and 20 female) groups to ensure an even distribution of individual male and female pups from all litters across the appropriately designated treatment groups. Adult and neonatal FA+PBS groups served as negative controls administered a placebo in the present study.

All animals were handled in accordance with standards established by the U.S. Animal Welfare Act in the National Institutes of Health Guidelines as well as those set forth by the University of California, Davis. Experiments and animal protocols were approved by the Institutional Animal Care and Use Committee at the University of California, Davis.

Environmental tobacco smoke (ETS) exposure

Mice were exposed for 6 weeks to FA (control) for 24 hr/day or ETS at a target concentration of 1 mg/m^3 for 6 hr/day, and 7 day/week (Figure 2). For ETS exposures, mice were placed in cages (6 mice/cage) in whole-body exposure chambers (0.44 m^3 capacity each) consisting of two cigarette handling and lighting devices, a metered puffing and flow machine, two dilution chimneys, one conditioning chamber, and a dilution and delivery system that distributed smoke equally within each chamber (Teague et al. 2008). For neonatal mice, this 6-week exposure spanned the last week of gestation through the first 5 weeks of life, for a pre- and post-natal exposure termed “perinatal exposure.” ETS-exposed mice were housed in an FA environment between each 6-hr exposure period. Control mice were kept in an animal room, in similar inhalation chambers ventilated with high-efficiency particulate air (HEPA)-FA. Measurements of total suspended particle (TSP), carbon monoxide (CO), and nicotine concentrations, as well as mean relative humidity and temperature, were taken from inside the exposure chamber every 30 min to ensure consistency. All chambers were maintained on a 12-hr light-dark cycle. At all times during the course of the experiment, mice had access to food and water *ad libitum*.

Research-grade cigarettes were purchased from the University of Kentucky for the ETS exposures and puffed by the smoke generation system under consistent smoking conditions (35-ml puff volume of two second duration, once per min). All research cigarettes were stored frozen and/or in the refrigerator prior to use. Cigarette packets were opened from the filter end of the cigarette and placed in a desiccation jar containing a 65% glycerin solution at the bottom to condition the cigarettes to the same level of humidity as the exposure room prior to combustion. ETS was formed by aging and diluting sidestream cigarette smoke and the mainstream puff volume with filtered air over a period of two min to achieve the target TSP concentration of 1 mg/m^3.

Influenza virus inoculation

The mouse-adapted viral strain, A/PR/8/34 H1N1 influenza (IAV), was generously donated by Dr. Melinda Beck at the University of North Carolina, Chapel Hill. The stock solution was diluted to individual doses of 12.6 $TCID_{50}$ in 40 μl PBS for inoculation. The $TCID_{50}$ (tissue culture infective dose) is the amount of virus required to kill 50% of infected hosts. Twenty-four hr after the final day of ETS/FA exposure, mice were inoculated with IAV or PBS (control) via nasal aspiration through both nares (approximately 20 μl/naris). The IAV dose was selected to be approximately 1000-fold lower than doses delivered in previous studies (Claude et al. 2012) to not overwhelm the animal with a heavy viral load. All mice were observed for signs of illness including unkempt fur, lethargy, shivering, and hunched posture daily (Claude et al. 2012). Seven days after inoculation, mice were euthanized with 0.2 ml Beuthanasia (65 mg/ml pentobarbital solution) by intraperitoneal (ip) injection for collection of BALF and tissue samples. The necropsy time-point, 7 days post infection, was based upon what has been reported as the peak time of influenza infection following IAV administration (Kim et al. 2017).

Collection and Examination of BALF

Each mouse was intratracheally cannulated for lung lavage. The complete lung was lavaged three times *in situ* with a single 0.6-ml aliquot of Hanks Balanced Salt Solution (HBSS) for BALF collection. BALF was centrifuged for 15 min at 1500g to separate the cellular and supernatant fractions. BALF cells were resuspended in 500 μl HBSS to determine total cell numbers using a hemocytometer. Cytospin slides were prepared using a Shandon Cytospin (Thermo Shandon, Inc., Pittsburg, PA), and stained with hematoxylin and eosin (H&E; American MasterTech, Lodi, CA) for cell differentials, which were assessed blindly *via* brightfield microscopy (Axiolab light microscope, Zeiss, Jena, Germany) for quantification of lymphocyte, neutrophil, and macrophage concentrations (500 cells/slide). Detailed explanations of the methods were described in a previous study (Castañeda and Pinkerton 2016).

Tissue collection and fixation

Left lungs were perfusion-fixed with 4% paraformaldehyde at 30 cm of hydrostatic pressure for 1 hr. The left lung from each animal was transversely cut into 4 equal slices and embedded in the same block of paraffin wax (Paraplast, Thermo Scientific). Several 5-μm thick sections of lung tissue were cut from each block using a Zeiss HM 355 rotary microtome (Carl Zeiss, Inc., Thornwood, NY) and placed on SuperFrost glass slides (one

section/slide; Fisher Scientific, Pittsburgh, PA) for histological or immunohistochemical analysis. The spleens of mice were collected and stored at −80 °C until further use.

Histology and light microscopy

Ten neonate (n=10/group; both males and females) and six adult (n=6/group; both males and females) mice were randomly selected for histological examination. One slide per animal was deparaffinized, rehydrated, stained with hematoxylin and eosin (H&E; American MasterTech, Lodi, CA), and viewed under the Zeiss Axiolab light microscope (Zeiss, Jena, Germany). No filter was used on the aperture, and the condenser lens was used to adjust focus and clarity. Images were captured using a Zeiss AxioCam ERc-5s (Zeiss, Jean, Germany) with full view of the entire lung lobe using a 5x objective lens. Since inflammation around airways and blood vessels was prevalent with IAV exposure alone (i.e., FA+IAV), a complete pan-analysis of the lung parenchyma was performed using a square lattice system to completely examine all lung lobes with Image J software (version 2.0.0; National Institutes of Health, Bethesda, MD). A step-by-step analysis of each square was performed to determine the presence of inflammatory cells including macrophages or polymorphonuclear cells (e.g., neutrophils and eosinophils). A positive (+) or negative (−) sign was assigned for each square with or without inflammatory cells, respectively. The total numbers of inflammation-positive and -negative squares were summed to calculate the percentage of the lung parenchyma with evidence of inflammation (% with inflammation = total (+) squares ÷ absolute total number of squares (+ and -) × 100). From this number, the mean percentage and standard error of the mean (SEM) were then determined for each treatment group. The graphs were created using the GraphPad Prism 7 program (GraphPad Software Inc., San Diego, CA).

Immunohistochemical analysis of T cell populations in the lungs

Three neonate and three adult mice were randomly selected from each treatment group for immunohistochemistry (IHC). The proportion of males to females was variable among the different groups. Three slides per animal were stained for IHC. Each of the three slides was stained with a different primary antibody. The antibodies included anti-CD4 (sc-7219, Santa Cruz Biotechnology, Santa Cruz, CA), anti-CD8 (ab22378, Abcam, Cambridge, MA), and anti-CD25 (MA5–12680, Invitrogen, Carlsbad, CA), which bind to the CD4, CD8, and CD25 membrane proteins of helper, cytotoxic, and regulatory T cells, respectively, and aid in their identification. The slides were deparaffinized in three changes of toluene (5, 2, and 2 min) and rehydrated in 100, 95, and 70% ethanol for 2 min each. Subsequently, slides were submerged in ethylenediaminetetraacetic acid and heated in a high-pressure decloaker for antigen retrieval. Endogenous peroxidase activity was blocked with 3% H_2O_2 for 10 min to avoid non-specific background staining. To eliminate non-specific binding of the primary antibody, the sections were incubated with protein block (Dako, Carpinteria, CA) for 10 min at room temperature (20 to 25°C). Each section was incubated for 1 hr at room temperature with one of the aforementioned primary antibodies, which were diluted in PBS with Tween® detergent at a ratio of 1:50 for anti-CD4, 1:200 for anit-CD8, and 1:1000 for anti-CD25 before use. Slide rinsing and incubation for 30 min at room temperature in horseradish peroxidase-labeled polymer anti-rabbit (EnVision System, catalog no. K4003, Dako) or anti-mouse (EnVision System, catalog no. K4001,

Dako) secondary antibody followed. Bound peroxidase activity was visualized with a 5-min incubation in a 3,3′-diaminobenzidine-positive substrate chromogen system (catalog no. K3468, Dako) according to the manufacturer's instructions. The tissue sections were counterstained with hematoxylin and cover slipped. Negative controls were treated with PBS instead of a primary antibody to confirm non-specific binding and false-positive results did not occur. Slides stained for CD4 or CD8 identification were evaluated blindly with a semi-quantitative scoring rubric (Table 1). For those stained for CD25 visualization were evaluated qualitatively.

Real-time quantitative reverse transcription-polymerase chain reaction analysis of splenic *IFN* isoforms

Nine neonate mice and 6 adult mice were randomly selected from each treatment group for real-time quantitative reverse transcription-polymerase chain reaction (RT-PCR) analysis. The ratio of males to females was 1:2 for neonates and 1:1 for adults. Total ribonucleic acid (RNA) was extracted from the spleen using a RNeasy kit with on-column DNase digestion (Qiagen, Valencia, CA) per the manufacturer's instructions. Reverse transcription of 1 μg DNA-free total RNA was carried out with 4 units of Omniscript Reverse Transcriptase (Qiagen, Valencia, CA), and 1 μM of oligo$(dT)_{15}$ primer in a final volume of 20 μl. Quantification of messenger RNA (mRNA) levels was done using the LightCycler System (Roche Diagnostics, Mannheim, Germany) with the QuantiTect SYBR Green PCR Kit (Qiagen, Valencia, CA) according to the manufacturer's instructions. The primers for each gene were selected from published sources [*IFN-a* (Riffault et al. 2000), *IFN-β* (Roth-Cross et al. 2007), *IFN-γ* (Maffei et al. 2004), *18S* (Roth-Cross et al. 2007)] and detailed in Table 2, herein. Data were analyzed with LightCycler software and quantified using the comparative threshold cycle (Ct) method (Pfaffl 2001) with mouse *18S* as a reference gene to serve as an internal control.

Statistical analysis

Group values were presented as arithmetic mean ± SEM. The normality of data distribution was evaluated with the Shapiro-Wilk test. Appropriate logarithmic or square root transformations were performed to obtain normal distributions before analysis of variance (ANOVA). Bonferroni corrections, based on the total number of comparisons for a given outcome, were applied to adjust for multiple comparisons. A two-way multivariate ANOVA with post hoc Tukey's multiple comparisons test was used to compare the differences between the experimental groups in GraphPad Prism software (GraphPad Prism 7, GraphPad Software Inc., San Diego, CA). A nonparametric test was selected when data were not normally distributed and could not be corrected by transformations. Statistical significance was accepted at a p-value < 0.05.

RESULTS

No mortality was observed in adult or neonatal mice up to the day of necropsy, 7 days after IAV inoculation.

ETS exposure

Inside exposure chambers, the concentrations averaged 1.01 ± 0.04 mg/m^3 for TSP, 7.04 ± 0.6 ppm for CO, and 0.11 ± 0.02 mg/m^3 for nicotine. The average relative humidity and temperature were 51.7 ± 8.08% and 71.4 ± 0.61°F, respectively.

Inflammatory effects observed in BALF

Lavage was performed for neonatal mice at 6 weeks of age (mean body weight 17.7 g) and young adult mice at 16 weeks of age (average body weight 22.9 g). The volume of fluid for bronchoalveolar lavage was adjusted, based upon body weight.

IAV inoculation significantly increased the number of total cells, macrophages, neutrophils, and lymphocytes in the BALF of FA- and ETS-exposed neonate groups relative to their virus-free (PBS-inoculated) counterparts (Figures 3a-3d). In adult mice, the ETS+IAV group exhibited significant elevation in numbers of total cells, neutrophils, and lymphocytes compared to the ETS+PBS and FA+IAV groups (Figures 3a, 3c, and 3d). A comparison of neonates and adults administered FA+IAV revealed that neonates displayed significantly greater total cell, macrophage, and neutrophil numbers (Figures 3a-3c).

Lung histopathology

Although neonatal mice appeared by histopathological analysis to have more inflamed lungs than similarly exposed adults, the results were not significant (Figure 4a). In addition, irrespective of the age at the time of exposure, inhalation of ETS+PBS did not significantly affect lung inflammation compared to FA+PBS for neonates and adults. The only significant changes observed were with IAV inoculation where such exposures resulted in significantly enhanced inflammation in lungs of neonatal and adult mice relative to their age-matched PBS-exposed counterparts (Figure 4a). Similarly, this was noted for groups previously exposed to FA for neonates and adult mice or ETS for neonates and adults. Significantly elevated inflammation was also observed between ETS+IAV and FA+IAV neonates (Figure 4a). This difference was not seen in ETS+IAV and FA+IAV adults. However, comparisons ETS+IAV- and FA+PBS-exposed groups showed increased lung inflammation in the former irrespective of age for neonates and adults Figure 4a), as observed by H&E staining (Figure 4b).

IHC analysis of T cell populations in lung tissue sections

In neonate and adult mice, FA+IAV versus FA+PBS exposure no significant effect was noted for CD4 helper and CD8 cytotoxic T cells in neonates and adult lungs (Figures 5a-5d). Irrespective of age, ETS+PBS exposure did not significantly alter recruitment of either T cell subset to the lungs compared to FA+PBS exposure (Figures 5a-5b).

In perinatally exposed mice alone, CD4 helper T cells were significantly increased as a result of ETS+IAV exposure compared to FA+PBS, ETS+PBS, and FA+IAV treatment (Figures 5a and c). No significant changes in CD4 T cells were observed upon ETS+IAV exposure in adult mice compared to FA+PBS, ETS+PBS, and FA+IAV exposure (Figures 5a and 5c). Rather, in adults, ETS+IAV versus FA+IAV treatment resulted in no significant alteration in pulmonary influx of CD4 T cells (Figures 5a and 5c). Cytotoxic CD8 T cells

did not alter significantly in neonates exposed to ETS+IAV versus FA+PBS or ETS+PBS illustrated in Figures 5b and 5d. In adults exposed to ETS+IAV, CD8 T cells numbers did not change markedly significantly when compared to same-age mice given FA+IAV (Figures 5b and 5d).

Number of CD25 increased as expected with viral infection versus PBS exposure in both neonatal and adult mouse groups previously exposed to FA or ETS (Figure 6).

RT-PCR of splenic *IFN* isoforms

Expression of *IFN-α*, *-β*, and *-γ* mRNA in the spleen of neonatal mice was significantly enhanced in the group exposed to ETS+IAV versus FA+PBS or ETS+IAV versus FA+IAV (Figure 7). In adult mice, gene expression of *IFN-γ* was significantly increased in the FA+IAV treatment group, as well as ETS+PBS group, compared to the FA+PBS group. Expression of *IFN-γ* was also significantly elevated in ETS+PBS-exposed adult mice relative to their neonate counterparts (Figure 7).

DISCUSSION

ETS exposure

The 1-mg/m^3 concentration was a measure of the total suspended particulate matter (TSP) in the ETS generated for the present study. The concentration of TSP in secondhand smoke may vary considerably based upon the number of smokers and the ventilation (air change) rate in the room in which smoking occurs. A single smoker might generate a surrounding cloud of particulates up to 2 mg/m^3 (IARC, 2004). Therefore, a caregiver who smokes might create such an atmosphere around a child. Although the TSP concentration used in the present study may be considered high, it is within the range of real-life exposures encountered by children and non-smoking adults. Before the enforced prohibition of smoking in public places, tobacco smoke particulate concentrations in bars approached several mg/m^3 (Repace et al. 2006; Hyland et al.2008).

Differences in body mass, lung size, and ventilatory patterns impact the exposure dose delivered to the lungs of lab animals and humans. Several investigators indicated that much higher gas and particle concentrations need to be used in small lab animal exposure studies to achieve the same dose as in humans (Snipes 1989; Hatch et al. 1994; Massaro 1997). The patterns of deposition, retention, and clearance for inhaled materials are different among different species, and responses and damage initiated by inhaled materials are also different (Snipes et al 1989). Dosimetry is further complicated in animals undergoing growth and development (Snipes et al 1989; Hatch et al. 1994). One limitation of the present study, and most other *in vivo* studies using mice/rats to model human inhalation exposures, is that the dose rates are not directly comparable even though the lung burden is similar.

ETS is composed of particles, gases, and vapors totaling more than 4,000 different constituents (Jenkins et al. 2000). The effects of ETS may be attributed to gases, vapors, and particles. The objective of the present study was to compare ETS exposures in mice during the perinatal (developmental) and young-adult life stages. Although it would be of interest to examine the comparative toxicity of an innocuous particle type, it is beyond the scope and

capabilities of this study. Future studies need to consider inclusion of an innocuous particle type as a negative control.

BALF and lung histopathology

While adult mice exposed to ETS+IAV had a far greater number of total BALF cells than their adult FA+IAV counterparts, virally infected neonatal mice showed significant increases in total BALF cells relative to their PBS-exposed counterparts irrespective of whether these animals were previously exposed to FA or ETS (Figure 3a). Data indicated that an exaggerated immune response might be triggered in neonatal mice by exposure to the virus alone (FA+IAV) or the combination of ETS+IAV. However, to mount the same severity of response in adult mice, it takes a combined (ETS+IAV) exposure. ETS+IAV exposure significantly increased infiltration of inflammatory cells, including neutrophils and lymphocytes, into the BALF of neonatal and adult mice compared to FA+PBS or ETS+PBS exposure (Figures 3b-3d). ETS+IAV treatment also elevated % lung covered by inflammation relative to FA+IAV in neonates and adults, but the effects were more severe in neonates (Figure 4). Outcomes of this investigation are in accordance with previous findings from the University of Melbourne, in which Gualano et al. (2008) concluded that smoke-induced activation of pro-inflammatory mediators did not protect against influenza infection, but rather worsened the immune response to the virus. The present findings and those of Gualano et al. (2008) are reasonable considering that ETS contains numerous chemicals, such as carbon monoxide, cadmium, and nitrogen oxides, that are harmful to the body.

The resistance of the FA+IAV adult mice group, but not neonates, to virally-induced inflammation (Figure 3) might be a result of immature immune systems of the neonates. You et al. (2008) concluded in their study that the adaptive immune system of younger mice was far weaker than that in older mice. Due to exposure to fewer pathogens, neonates, who have not been exposed to as many diseases, have immature adaptive immune systems, notably with fewer developed adaptive T cells (You et al. 2008; Simon et al 2015). This is supported in the present study by the innately skewed immune response where lower number of influxing lymphocytes and higher number of resident macrophages in the BALF were detected in neonatal mice in comparison to adults (Figure 3). Coates et al (2015) demonstrated that antigen-presenting cells (e.g., macrophages) in the pediatric innate immune system tend to be less stimulatory when challenged with Toll-like receptor (TLR) agonists, which dampened responses leading to decreased antigen presentation and T cell co-stimulation relative to adults. Neutrophil generation of reactive oxygen species (ROS) and extracellular traps, which enable neutrophils to bind and kill pathogens, was also noted to be reduced in neonates compared to adults (Lawrence et al 2017). These immature adaptive responses characteristic of a developing immune system also contribute to the increased morbidity of children upon infection with influenza. Overall, the outcomes indicate that because the neonatal adaptive immune system lacks some of the benefits of successfully combating prior pathogenic challenges (e.g., memory T cells and B cells), immune responses to viral (e.g., IAV) infection are compensatively skewed toward non-specific innate defenses. In adult mice perhaps, prior ETS exposure weakened the immune

system and enhanced susceptibility, inducing as large an influx of immune cells as seen in the neonates (Figures 3 and 4).

Pulmonary influxes of CD4, CD8, and CD25 T cells

Semi-quantitative analysis of CD4 and CD8 T cell populations in the lungs yielded similar patterns of pulmonary influx. While perinatal ETS+IAV exposure was associated with a steep rise in CD4 Helper T cells relative to all other treatments, no marked change in CD4 cell influx was detected in adults. General CD8 T cell responses in neonates and adults were similar to those for CD4 cells and did not attain significance (Figure 5b).

In general, CD4 and CD8 T cells are a normal part of an antiviral immune response (Sun and Braciale 2013). CD4 cells participate in myriad protective immunity pathways to fight against viruses (Sant and McMichael 2012). Their functions include but are not limited to recruiting key lymphoid cell populations, providing help for other effector cells, and producing cytokines or cell-mediated cytotoxicity directly. Exaggerated CD4 responses were observed in ETS+IAV-exposed neonates in the present study which might lead to hyperinflammation and lung injury over time. A significantly lower level of *IFN-γ* was also found in the spleens of ETS+PBS-treated neonates compared to ETS+PBS-treated adult mice. These findings help to explain why neonates exhibit greater susceptiblity to respiratory virus infection and severe outcomes relative to adults.

Unlike CD4 T cells, CD8 T cells play roles in producing cytokines (e.g., *IFN-γ*, TNF, and degranulates) to mediate viral clearance (Schmidt and Varga 2018). In the present study, the number of CD8-positive T cells was not markedly altered in lungs and airways of neonate and adult mice as a result of IAV, versus PBS, inoculation (Figures 5a and 5b). The reason for the lack of significance may be attributed to in this study compared to Schmidt and Varga (2018) might be due to kinetics. There is a delay in pulmonary influx of virus-specific CD8 T cells, such that they peak in number approximately 10 days following respiratory IAV infections. In the current study, necropsies were conducted at day 7 post IAV exposure suggesting the number of CD8 cells in the lungs had not peaked.

CD8 cell impairment upon viral infection may be another reason for non-significant influx observed with IAV- versus PBS-inoculation. Previous investigators showed that following influenza virus infection, a classic antiviral response occurs, with activated CD4 and CD8 T cells, macrophages, dendritic cells, and other cell types (Smed-Sörensen et al. 2012; He et al. 2017; Pizzolla et al. 2017). However, T cell impairment, initiated by inhibiting survival or function of specific CD8 cells, is a necessary defense for the host to prevent excessive immune-mediated damage during viral acute lung infection, and preserve healthy lung tissue (Rogers and Williams 2019). Cheemarla et al (2019) examined the effects of human respiratory syncytial virus (hRSV) infection after prenatal ETS exposure and noted that although respiratory inflammation was exacerbated by hRSV infection, viral clearance was delayed, and the hRSV-specific CD8 T cell response was decreased relative to only hRSV-infected neonatal mice. This latter finding lends support to the idea that host CD8 cell impairment may have occurred in IAV-exposed groups in the present study.

One mechanism of CD8 cell impairment is inhibition by CD25 T cells. Regulatory CD25 T cells play a key role in balancing lung inflammation and minimizing tissue injuries resulting from immune responses (Fulton et al 2010) by directly or indirectly inhibiting the functions of not just CD8 cells, but also CD4 T cells, B cells, dendritic cells, and natural killer cells (Rouse et al 2006). IAV was expected, in the present study, to directly weaken the function of both (CD4 and CD8) effector T cell types (Bedoya et al. 2013; Brincks et al. 2013) through induction of CD25 T cells, but this did not appear to be the case when compared to PBS. Similar to the significant and non-significant findings for CD4 and CD8 T cells, CD25 T cells appeared to be elevated in the lung tissues of the IAV- versus PBS-exposed groups (Figure 6). Treg cells were found in the murine lung up to 6 weeks after acute IAV infection (Kraft et al. 2013), a range that includes the IAV incubation period (7 days) used in the present study.

When viewed as a whole, the results from the IHC experiment also indicated an enhanced inflammatory response in neonates with ETS+IAV, which was not seen in adults (Figures 5a-5b). ETS+IAV exposure during adulthood exerted no significant effect on CD4 and CD8 T cell concentrations in the lungs. Taken together findings found in adult mice indicate an ability of ETS to diminish the adaptive immune responses in general, which might lead to worse clinical outcomes (Strzelak et al. 2018). Despite that the mechanisms driving the present results require further research, at least two studies lend credence to our findings. T cell proliferation and T cell receptor signaling were reported by Geng et al. (1995) to be impaired after adding tobacco extracts to cell cultures, and ETS exposure was demonstrated by Feng et al. (2011) to inhibit the pulmonary CD4 and CD8 T cell responses and T cell receptor production of *IFN-γ* in adult mice infected with influenza virus.

mRNA expression of *IFN* isoforms

Findings by Feng et al. (2011) support those of the present study in which there was no significant difference in the mRNA expression of *IFN-α, β* and *γ* in the spleens of adult mice with exposure to ETS+IAV versus FA+PBS (Figure 7). On the other hand, in neonatal mice, mRNA expression of *IFN-α, β* and *γ* in the spleen showed a significant difference with ETS+IAV treatment compared to FA+PBS or FA+IAV (Figure 7). In addition to CD4 T cells in neonates after exposure to ETS and virus elevated compared with those in adults, all of these support that perinatal exposure to ETS makes neonates more susceptible to influenza virus with exaggerated immune responses compared to adults.

An enhancement in adaptive immune functions as evidenced by increased *IFN* expression might be interpreted as therapeutic and protective given the improved anti-viral response to influenza (Davidson et al. 2016). Previously Haasbach et al. 2011 reported that *IFN* treatment increased the secretion of antiviral cytokines that mediate the decrease of influenza virus in the lung. Yoo et al (2010) noted that *IFN* treatment effectively controlled viral replication and immunopathology, resulting in viral clearance in infected lung tissues. Weiss et al (2010) demonstrated that *IFN* treatment cleared the virus and decreased inflammation by reducing the number of T cells and NKT cells in infected lungs.

One limitation in our RT-PCR data was that we did not run gel electrophoresis was not run to confirm the specificity and amplification efficiencies of the primers. The primers

for each gene were selected from published sources and analyzed and confirmed by gel electrophoresis in those studies (Riffault et al. 2000, Roth-Cross et al. 2007, Maffei et al. 2004). It is conceivable that RT-PCR results are reliable because the amplicon sizes for *IFN-α*, *-β*, and *-γ* were less than 300, and Ct values were less than 30. In future experiments, gel electrophoresis will be included to reduce the potential risk of mismatches, cross-matches, co-amplifications, and suboptimal amplicon sizes.

BALF (Figure 3) and histopathology (Figure 4) findings in this study suggest viral infection is a major driver of inflammation in both neonates and adults. However, striking differences were noted between the two life stages. These differences included significantly enhanced phagocytic (Figure 3b) and lymphocytic (Figure 3d) inflammation in neonates versus adults with ETS+IAV exposure; and a neonate-specific finding of significantly more CD4+ lymphocytes with ETS+IAV versus FA+IAV exposure (Figure 5a) in neonates versus adults. Other neonate-specific findings included significantly increased splenic *IFN-α* (Figure 7a); *IFN-β* (Figure 7b), and *IFN-γ* (Figure 7c) mRNA levels with ETS+IAV versus FA+IAV exposure. Given that macrophages produce *IFN-α*, *-β*, and *-γ* and activate CD4 cells (Figure 1), the findings in the present study suggest that although neonate and adult mice are both susceptible to viral infection, early life exposure to ETS may have promoted stronger macrophage-specific responses in the neonates versus adults.

CONCLUSIONS

Our data demonstrated that the timing of ETS exposure differentially impacts inflammation and immune cell recruitment to lungs during IAV infection. A significantly elevated inflammatory response in the lungs of neonatal and adult mice when challenged with IAV versus PBS was found. However, neonatal mice compared to adult mice exhibited a significantly greater degree of inflammation when previously challenged by ETS versus FA exposure. In addition, a significantly higher production of type I and III IFNs was detected in the spleen of neonatal mice compared with adults with ETS+IAV versus FA+IAV or FA+PBS exposure. These findings suggest neonatal exposure to ETS displays the potential to enhance pulmonary and systemic innate immune responses to overwhelm the more protective anti-inflammatory defenses in adults against IAV. Thus, early life stage exposure ETS has the potential to increase the incidence and severity of respiratory influenza virus infection in infants compared to adults. With the continued high prevalence of childhood respiratory viral infection and exposure to tobacco combustion products, future research would help to better elucidate those underlying mechanisms as a means to reduce the incidence of respiratory influenza viral infection in infants exposed to ETS during early life.

ACKNOWLEDGEMENTS

The authors thank Alexa K. Pham, Jocelyn A. Claude, and Dale L. Uyeminami for technical laboratory assistance during the course of this study.

FUNDING

This research was supported by the Centers for Disease Control and Prevention/National Institute of Occupational Safety and Health grant CDC/NIOSH U54 OH07550 and the National Institute of Environmental Health Sciences (NIEHS) grants P30 ES023513, and P51 OD011107.

REFERENCES

Bedoya F, Cheng G-S, Leibow A, Zakhary N, Weissler K, Garcia V, Aitken M, et al. 2013. Viral antigen induces differentiation of Foxp3+ natural regulatory T cells in influenza virus-infected mice. J. Immunol 190 :6115–6125. doi:10.4049/jimmunol.1203302. [PubMed: 23667113]

Brincks EL, Roberts AD, Cookenham T, Sell S, Kohlmeier JE, Blackman MA, and Woodland DL 2013. Antigen-specific memory regulatory CD4+Foxp3+ T cells control memory responses to influenza virus infection. J. Immunol 190:3438–3446. doi:10.4049/jimmunol.1203140. [PubMed: 23467933]

Cao J, Xu X, Hylkema MN, Zeng EY, Sly PD, Suk WA, Bergman Å, and Huo X 2016. Early-life exposure to widespread environmental toxicants and health risk: A focus on the immune and respiratory systems. Ann. Glob. Health 82: 119–131. doi:10.1016/j.aogh.2016.01.023. [PubMed: 27325070]

Castañeda AR, and Pinkerton KE 2016. Investigating the effects of particulate matter on house dust mite and ovalbumin allergic airway inflammation in mice. Curr Protoc Toxicol 68:18.1–18.18.18. doi:10.1002/cptx.5. [PubMed: 27145110]

Centers for Disease Control and Prevention (CDC). 2014. The health consequences of smoking-50 years of progress: A report of the surgeon general. NBK179276, U.S. Department of Health and Human Services, Centers for Disease Control and Prevention, National Center for Chronic Disease Prevention and Health Promotion, Office on Smoking and Health, Atlanta, GA. Accessed October 14, 2020. https://www.ncbi.nlm.nih.gov/books/NBK179276/.

Centers for Disease Control and Prevention (CDC). 2020. Children and Secondhand Smoke Exposure Office on Smoking and Health, National Center for Chronic Disease Prevention and Health Promotion, Atlanta, GA. Accessed September 21, 2021. https://www.cdc.gov/tobacco/basic_information/secondhand_smoke/children-home/.

Cheemarla NR, Uche IK, McBride K, Naidu S, and Guerrero-Plata A 2019. In utero tobacco smoke exposure alters lung inflammation, viral clearance, and CD8+ T-cell responses in neonatal mice infected with respiratory syncytial virus. Am. J. Physiol. Lung Cell. Mol. Physiol 317: L212–L221. doi:10.1152/ajplung.00338.2018. [PubMed: 31090436]

Claude JA, Grimm A, Savage HP, and Pinkerton KE 2012. Perinatal exposure to environmental tobacco smoke (ETS) enhances susceptibility to viral and secondary bacterial infections. Int. J. Environ. Res. Public Health 9: 3954–3964. doi:10.3390/ijerph9113954. [PubMed: 23202826]

Coates BM, Staricha KL, Wiese KM, and Ridge KM 2015. Influenza A virus infection, innate immunity, and childhood. JAMA Pediatr 169: 956–963. doi:10.1001/jamapediatrics.2015.1387. [PubMed: 26237589]

Colonna M, Krug A, and Cella M 2002. Interferon-producing cells: On the front line in immune responses against pathogens. Curr Opin Immunol 14:373–379. doi:10.1016/S0952-7915(02)00349-7. [PubMed: 11973137]

Corthay A 2009. How do regulatory T cells work? Scand J Immunol 70: 326–336. Doi: 10.1111/j.1365-3083.2009.02308.x. [PubMed: 19751267]

Davidson S, McCabe TM, Crotta S, Gad HH, Hessel EM, Beinke S, Hartmann R, and Wack A 2016. IFN lambda is a potent anti-influenza therapeutic without the inflammatory side effects of IFN alpha treatment. EMBO Mol Med 8: 1099–1112. doi:10.15252/emmm.201606413. [PubMed: 27520969]

Feng Y, Kong Y, Barnes PF, Huang F-F, Klucar P, Wang X, Samten B, et al. 2011. Exposure to cigarette smoke inhibits the pulmonary T-cell response to influenza virus and *Mycobacterium tuberculosis*. Infect. Immun 79: 229–237. doi:10.1128/IAI.00709-10. [PubMed: 20974820]

Fernández-Plata R, Rojas-Martínez R, Martínez-Briseño D, García-Sancho C, and Pérez-Padilla R 2016. Effect of passive smoking on the growth of pulmonary function and respiratory symptoms in schoolchildren. Rev. Invest. Clin 68:119–127. [PubMed: 27408998]

Fulton RB, Meyerholz DK, and Varga SM 2010. Foxp3+ CD4 regulatory T cells limit pulmonary immunopathology by modulating the CD8 T cell response during respiratory syncytial virus infection. J. Immunol 185:382–392. doi:10.4049/jimmunol.1000423.

Geng YM, Savage SM, Johnson LJ, Seagrave J, and Sopori ML 1995. Effects of nicotine on the immune response. I. Chronic exposure to nicotine impairs antigen receptor-mediated signal transduction in lymphocytes. Toxicol. Appl. Pharmacol 135: 268–728. doi:10.1006/taap.1995.1233. [PubMed: 8545837]

Gualano RC, Hansen MJ, Vlahos R, Jones JE, Park-Jones RA, Deliyannis G, Turner SJ, Duca KA, and Anderson GP 2008. Cigarette smoke worsens lung inflammation and impairs resolution of influenza infection in mice. Respir. Res 9: 53. doi:10.1186/1465-9921-9-53. [PubMed: 18627612]

Haasbach E, Droebner K, Vogel AB, and Planz O 2011. Low-dose interferon Type I treatment is effective against H5N1 and swine-origin H1N1 influenza A viruses in vitro and in vivo. J Interferon Cytokine Res 31:515–525. doi:10.1089/jir.2010.0071. [PubMed: 21323570]

Han SG, Bhoopalan V, Akinbiyi T, Gairola CG, and Bhalla DK 2011. In utero tobacco smoke exposure alters pulmonary responses of newborn rats to ozone. J. Toxicol. Environ. Health A 74 : 668–677. doi:10.1080/15287394.2011.539133. [PubMed: 21432716]

Hanson ML, Holásková I, Elliott M, Brundage KM, Schafer R, and Barnett JB 2012. Prenatal cadmium exposure alters postnatal immune cell development and function. Toxicol. Appl. Pharmacol 261:196–203. doi:10.1016/j.taap.2012.04.002. [PubMed: 22521604]

Hatch GE, Slade R, Harris LP, McDonnell WF, Devlin RB, Koren HS, Costa DL, McKee J 1994. Ozone dose and effect in humans and rats. A comparison using oxygen-18 labeling and bronchoalveolar lavage. Am. J. Respir. Crit. Care Med 150: 676–683. doi:10.1164/ajrccm.150.3.8087337. [PubMed: 8087337]

He W, Chen C-J, Mullarkey CE, Hamilton JR, Wong CK, Leon PE, Uccellini MB, et al. 2017. Alveolar macrophages are critical for broadly-reactive antibody-mediated protection against influenza A virus in mice. Nat. Commun 8: 846. doi:10.1038/s41467-017-00928-3. [PubMed: 29018261]

Hollams EM, de Klerk NH, Holt PG, and Sly PD 2014. Persistent effects of maternal smoking during pregnancy on lung function and asthma in adolescents. Am J Respir Crit Care Med 189: 401–407. doi: 10.1164/rccm.201302-0323OC. [PubMed: 24251622]

Holmes LM and Ling PM 2017. Workplace secondhand smoke exposure: A lingering hazard for young adults in California. Tob. Control 26: e79–84. doi:10.1136/tobaccocontrol-2016-052921. [PubMed: 27417380]

Hufford MM, Kim TS, Sun J, and Braciale TJ 2015. The effector T cell response to influenza infection. Curr. Top. Microbiol. Immunol 386:423–455. doi:10.1007/82_2014_397. [PubMed: 25033753]

Hyland A, Travers MJ, Dresler C, Higbee C, Cummings KM 2008. A 32-country comparison of tobacco smoke derived particle levels in indoor public places. Tob. Control 17:159–165. doi: 10.1136/tc.2007.020479 [PubMed: 18303089]

IARC Working Group on the Evaluation of Carcinogenic Risks to Humans. 2004. Tobacco smoke and involuntary smoking. Lyon (FR): International Agency for Research on Cancer (IARC Monographs on the Evaluation of Carcinogenic Risks to Humans, No. 83.) 1, Composition, Exposure and Regulations. Accessed October 24, 2021. https://www.ncbi.nlm.nih.gov/books/NBK316410/.

Ilyushina NA, Khalenkov AM, Seiler JP, Forrest HL, Bovin NV, Marjuki H, Barman S, Webster RG, and Webby RJ 2010. Adaptation of pandemic H1N1 influenza viruses in mice. J. Virol 84: 8607–8616. doi:10.1128/JVI.00159-10. [PubMed: 20592084]

Jenkins RA, Tomkins B, Guerin MR 2000. The Chemistry of Environmental Tobacco Smoke: Composition and Measurement (2nd ed.). CRC Press. doi:10.1201/9781482278651.

Kamal RP, Katz JM, and York IA 2014. Molecular determinants of influenza virus pathogenesis in mice. Curr. Top. Microbiol. Immunol 385:243–724. doi:10.1007/82_2014_388. [PubMed: 25038937]

Kim S, Kim MJ, Kim CH, Kang JW, Shin HK, Kim DY, Won TB, Han DH, Rhee CS, Yoon JH, Kim HJ 2017. The superiority of IFN-λ as a therapeutic candidate to control acute influenza viral lung infection. Am J Respir Cell Mol Biol 56: 202–212. doi:10.1165/rcmb.2016-0174OC. [PubMed: 27632156]

Kraft ARM, Wlodarczyk MF, Kenney LL, and Selin LK 2013. PC61 (anti-CD25) treatment inhibits influenza A virus-expanded regulatory T cells and severe lung pathology during a subsequent heterologous lymphocytic choriomeningitis virus infection. J. Virol 87: 12636–12647. doi:10.1128/JVI.00936-13. [PubMed: 24049180]

Kubota K, and Kadoya Y 2011. Innate IFN-gamma-producing cells in the spleen of mice early after Listeria monocytogenes infection: importance of microenvironment of the cells involved in the production of innate IFN-gamma. Front Immunol 2:26. doi:10.3389/fimmu.2011.00026. [PubMed: 22566816]

Lawrence SM, Corriden R, and Nizet V 2017. Age-appropriate functions and dysfunctions of the neonatal neutrophil. Front. Pediatr 5:23. doi:10.3389/fped.2017.00023. [PubMed: 28293548]

Lee F, and Lawrence DA 2018. From infections to anthropogenic inflicted pathologies: Involvement of immune balance. J Toxicol Environ Health B 21: 24–46.

Lee PN, Forey BA, Coombs KJ, Hamling JS, and Thornton AJ 2018. Epidemiological evidence relating environmental smoke to COPD in lifelong non-smokers: A systematic review. F1000Res 7:146. doi:10.12688/f1000research.13887.3. [PubMed: 32089819]

Maffei CML, Mirels LF, Sobel RA, Clemons KV, and Stevens DA 2004. Cytokine and inducible nitric oxide synthase mRNA expression during experimental murine cryptococcal meningoencephalitis. Infect Immunity 72: 2338–2349. doi:10.1128/IAI.72.4.2338-2349.2004. [PubMed: 15039359]

Massaro EJ (Ed.). 1997. Handbook of Human Toxicology (1st ed.). CRC Press. doi:10.1201/9781439805756.

Miller JL, and Anders EM 2003. Virus-cell interactions in the induction of type 1 interferon by influenza virus in mouse spleen cells. J. Gen. Virol 84: 193–202. doi:10.1099/vir.0.18590-0. [PubMed: 12533716]

Noakes PS, Holt PG, and Prescott SL 2003. Maternal smoking in pregnancy alters neonatal cytokine responses. Allergy 58:1053–1058. doi:10.1034/j.1398-9995.2003.00290.x. [PubMed: 14510725]

Nooshinfar E, Bashash D, Abbasalizadeh M, Safaroghli-Azar A, Sadreazami P, and Esmaeil Akbari M 2017. The molecular mechanisms of tobacco in cancer pathogenesis. Int. J. Cancer Manage 10: e7902. doi:10.17795/ijcp-7902.

Pacheco SA, Torres VM, Louro H, Gomes F, Lopes C, Marçal N, Fragoso E, et al. 2013. Effects of occupational exposure to tobacco smoke: Is there a link between environmental exposure and disease? J. Toxicol. Environ. Health A 76:311–327. doi:10.1080/15287394.2013.757269. [PubMed: 23514073]

Pfaffl MW 2001. A new mathematical model for relative quantification in real-time RT-PCR. Nucl Acids Res29: e45–e45. doi:10.1093/nar/29.9.e45. [PubMed: 11328886]

Pizzolla A, Nguyen THO, Smith JM, Brooks AG, Kedzierska K, Heath WR, Reading PC, and Wakim LM 2017. Resident memory CD8+ T cells in the upper respiratory tract prevent pulmonary influenza virus infection. Sci. Immunol 2: eaam6970. doi:10.1126/sciimmunol.aam6970. [PubMed: 28783656]

Price GE, Gaszewska-Mastarlarz A, and Moskophidis D 2000. The role of alpha/beta and gamma interferons in development of immunity to influenza A virus in mice. J. Virol 74: 3996–4003. doi:10.1128/jvi.74.9.3996-4003.2000. [PubMed: 10756011]

Radigan KA, Misharin AV, Chi M, and Budinger GS 2015. Modeling human influenza infection in the laboratory. Infect Drug Resist 8: 311–320. doi:10.2147/IDR.S58551. [PubMed: 26357484]

Repace JL, Hyde JN, Brugge D 2006. Air pollution in Boston bars before and after a smoking ban. BMC Public Health 6: 266. do:10.1186/1471-2458-6-266. [PubMed: 17069654]

Riffault S, Carrat C, Milon G, Charley B, and Colle JH 2000. Transient IFN-γ synthesis in the lymph node draining a dermal site loaded with UV-irradiated herpes simplex virus type: An NK- and CD3-dependent process regulated by IL-12 but not by IFN-α/β. J Gen Virol 81: 2365–2373. doi:10.1099/0022-1317-81-10-2365. [PubMed: 10993924]

Rogers MC and Williams JV 2019. Reining in the CD8+ T cell: Respiratory virus infection and PD-1-mediated T-cell impairment. PLoS Pathog 15: e1007387. doi:10.1371/journal.ppat.1007387. [PubMed: 30605483]

Rosendahl Huber S, van Beek J, de Jonge J, Luytjes W, and van Baarle D 2014. T cell responses to viral infections - opportunities for peptide vaccination. Front Immunol 5:171. doi: 10.3389/fimmu.2014.00171. [PubMed: 24795718]

Roth-Cross JK, Martínez-Sobrido L, Scott EP, García-Sastre A, and Weiss SR 2007. Inhibition of the alpha/beta interferon response by mouse hepatitis virus at multiple levels. J. Virol 81: 7189–7199. doi:10.1128/JVI.00013-07. [PubMed: 17459917]

Rouse BT, Sarangi PP, and Suvas S 2006. Regulatory T cells in virus infections. Immunol. Rev 212: 272–286. doi:10.1111/j.0105-2896.2006.00412.x. [PubMed: 16903920]

Sant AJ and McMichael A 2012. Revealing the role of CD4(+) T cells in viral immunity. J. Exp. Med 209:1391–1395. doi:10.1084/jem.20121517. [PubMed: 22851641]

Sant AJ, DiPiazza AT, Nayak JL, Rattan A, and Richards KA 2018a. CD4 T cells in protection from influenza virus: Viral antigen specificity and functional potential. Immunol. Rev 284 :91–105. doi:10.1111/imr.12662. [PubMed: 29944766]

Sant AJ, Richards KA, and Nayak J 2018b. Distinct and complementary roles of CD4 T cells in protective immunity to influenza virus. Curr. Opin. Immunol 53:13–21. doi:10.1016/j.coi.2018.03.019. [PubMed: 29621639]

Schmidt ME and Varga SM 2018. The CD8 T cell response to respiratory virus infections. Front. Immunol 9: 678. doi:10.3389/fimmu.2018.00678. [PubMed: 29686673]

Simon AK, Hollander GA, and McMichael A 2015. Evolution of the immune system in humans from infancy to old age. Proc. Roy. Soc 282: 20143085. doi:10.1098/rspb.2014.3085.

Singh SP, Gundavarapu S, Peña-Philippides JC, Rir-Sima-ah J, Mishra NC, Wilder JA, Langley RJ, Smith KR, and Sopori ML 2011. Prenatal secondhand cigarette smoke promotes Th2 polarization and impairs goblet cell differentiation and airway mucus formation. J. Immunol 187:4542–4552. doi:10.4049/jimmunol.1101567. [PubMed: 21930963]

Smed-Sörensen A, Chalouni C, Chatterjee B, Cohn L, Blattmann P, Nakamura N, Delamarre L, and Mellman I 2012. Influenza A virus infection of human primary dendritic cells impairs their ability to cross-present antigen to CD8 T Cells. PLoS Pathog 8: e1002572. doi:10.1371/journal.ppat.1002572. [PubMed: 22412374]

Snipes MB 1989. Long-term retention and clearance of particles inhaled by mammalian species. CRC Crit. Rev. Toxicol 20:175–211. doi:10.3109/10408448909017909.

Snipes MB, McClellan RO, Mauderly JL, Wolff RK 1989. Retention patterns for inhaled particles in the lung: comparisons between laboratory animals and humans for chronic exposures. Health Phys 17(Suppl 1): 69–77. doi:10.1097/00004032-198907001-00008.

Strzelak A, Ratajczak A, Adamiec A, and Feleszko W 2018. Tobacco smoke induces and alters immune responses in the lung triggering inflammation, allergy, asthma and other lung diseases: A mechanistic review. Int. J. Environ. Res. Public Health 15: doi:10.3390/ijerph15051033.

Sumino K, Tucker J, Shahab M, Jaffee KF, Visness CM, Gern JE, Bloomberg GR, and Holtzman MJ 2012. Antiviral IFN-γ responses of monocytes at birth predict respiratory tract illness in the first year of life. J. Allergy Clin. Immunol 129: 1267–1273.e1. doi:10.1016/j.jaci.2012.02.033. [PubMed: 22460071]

Sun J, and Braciale TJ 2013. Role of T cell immunity in recovery from influenza virus infection. Curr Opin Virol 3: 425–429. doi:10.1016/j.coviro.2013.05.001. [PubMed: 23721865]

Teague SV, Pinkerton KE, Goldsmith M, Gebremichael A, Chang S, Jenkins RA, and Moneyhun JH 2008. Sidestream cigarette smoke generation and exposure system for environmental tobacco smoke studies. Inhal Toxicol 6: 79–93.

Thompson WW, Shay DK, Weintraub E, Brammer L, Bridges CB, Cox NJ, and Fukuda K 2004. Influenza-Associated Hospitalizations in the United States. J Am Med Assoc 292:1 333–1340. doi: 10.1001/jama.292.11.1333.

Thompson WW, Weintraub E, Dhankhar P, Cheng P-Y, Brammer L, Meltzer MI, Bresee JS, and Shay DK 2009. Estimates of US influenza-associated deaths made using four different methods. Influenza Other Respir. Viruses 3: 37–49. doi:10.1111/j.1750-2659.2009.00073.x. [PubMed: 19453440]

Torres LHL, Moreira WL, Garcia RCT, Annoni R, Carvalho ALN, Teixeira SA, Pacheco-Neto M, et al. 2012. Environmental tobacco smoke induces oxidative stress in distinct brain regions of infant

mice. J. Toxicol. Environ. Health A 75: 971–980. doi:10.1080/15287394.2012.695985. [PubMed: 22852847]

Weiss ID, Wald O, Wald H, Beider K, Abraham M, Galun E, Nagler A, and Peled A 2010. IFN-gamma treatment at early stages of influenza virus infection protects mice from death in a NK cell-dependent manner. J Interferon Cytokine Res 30:439–449. doi:10.1089/jir.2009.0084. [PubMed: 20235626]

Xu X, Blanton L, Elal AIA, Alabi N, Barnes J, Biggerstaff M, Brammer L, et al. 2019. Update: Influenza activity in the United States during the 2018–19 season and composition of the 2019–20 influenza vaccine. MMWR 68: 544–551. doi:10.15585/mmwr.mm6824a3. [PubMed: 31220057]

Ygberg S and Nilsson A 2012. The developing immune system – from foetus to toddler. Acta Paediatr 101: 120–127. doi:10.1111/j.1651-2227.2011.02494.x. [PubMed: 22003882]

Yoo JK, Baker DP, and Fish EN 2010. Interferon-beta modulates type 1 immunity during influenza virus infection. Antiviral Res 88: 64–71. doi: 10.1016/j.antiviral.2010.07.006. [PubMed: 20659503]

You D, Ripple M, Balakrishna S, Troxclair D, Sandquist D, Ding L, Ahlert TA, and Cormier SA Inchoate CD8+ T cell responses in neonatal mice permit influenza-induced persistent pulmonary dysfunction. J. Immunol 181: 3486–3494. doi:10.4049/jimmunol.181.5.3486. [PubMed: 18714021]

Yu M, Zheng X, Peake J, Joad JP, and Pinkerton KE 2008. Perinatal environmental tobacco smoke exposure alters the immune response and airway innervation in infant primates. J. Allergy Clin. Immunol 122: 640–647.e1. doi:10.1016/j.jaci.2008.04.038. [PubMed: 18571708]

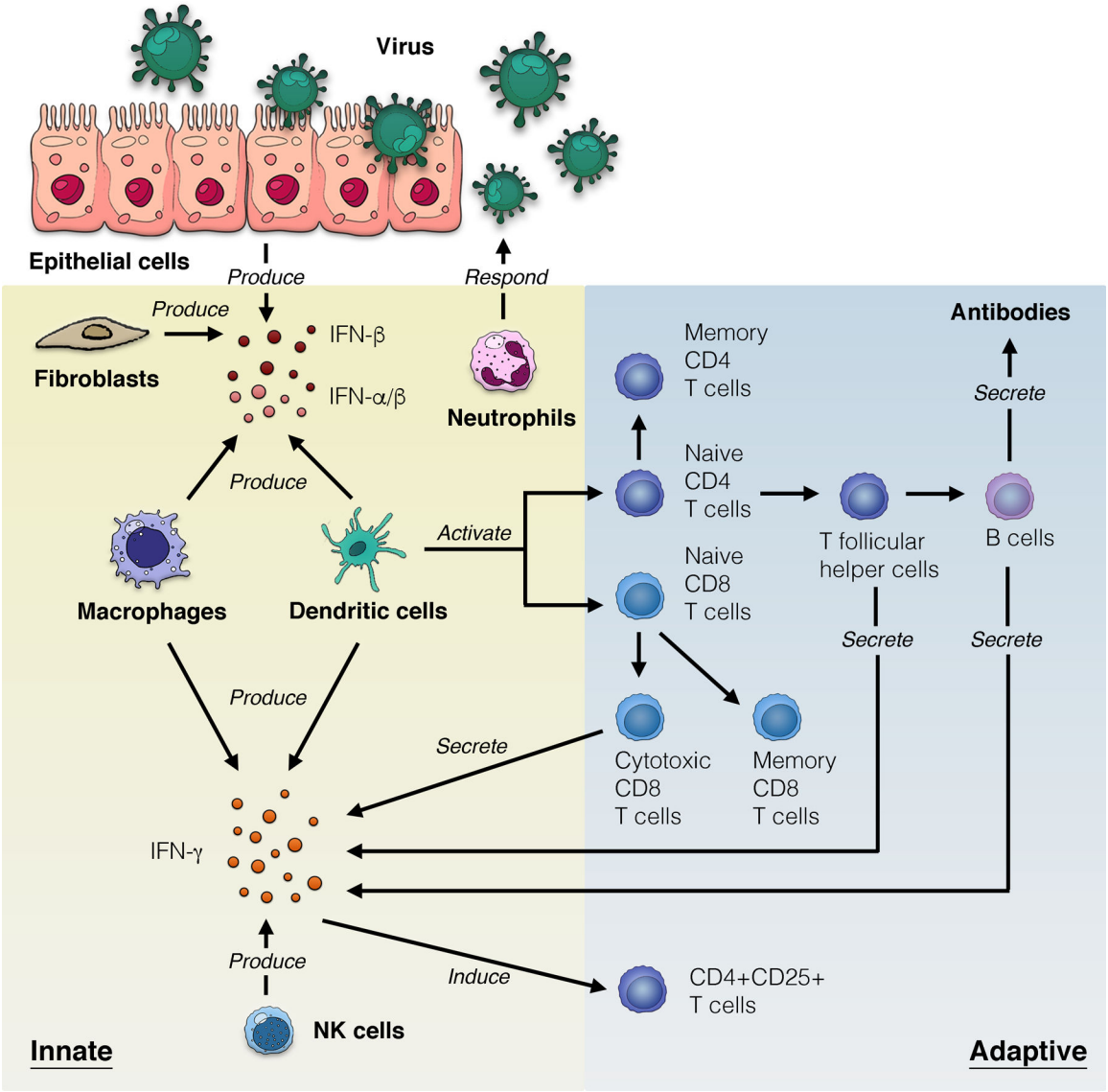

Figure 1. Normal *IFN-α, β,* and *γ* innate and adaptive immune responses.

Innate immune cells, such as macrophages and dendritic cells, produce *IFN-α* and *β* after sensing pathogen components. Non-immune cells, such as fibroblasts and epithelial cells, predominantly produce *IFN-β*. Macrophages, dendritic cells, and natural killer cells have been reported to produce *IFN-γ*. For the adaptive immunity, *IFN-α* and *β* can augment antibody production by B cells and amplify the effector function of T cells. *IFN-γ* is secreted by helper T cells, CD8 T cells, and B cells, which can induce CD4+CD25+ regulatory T cells.

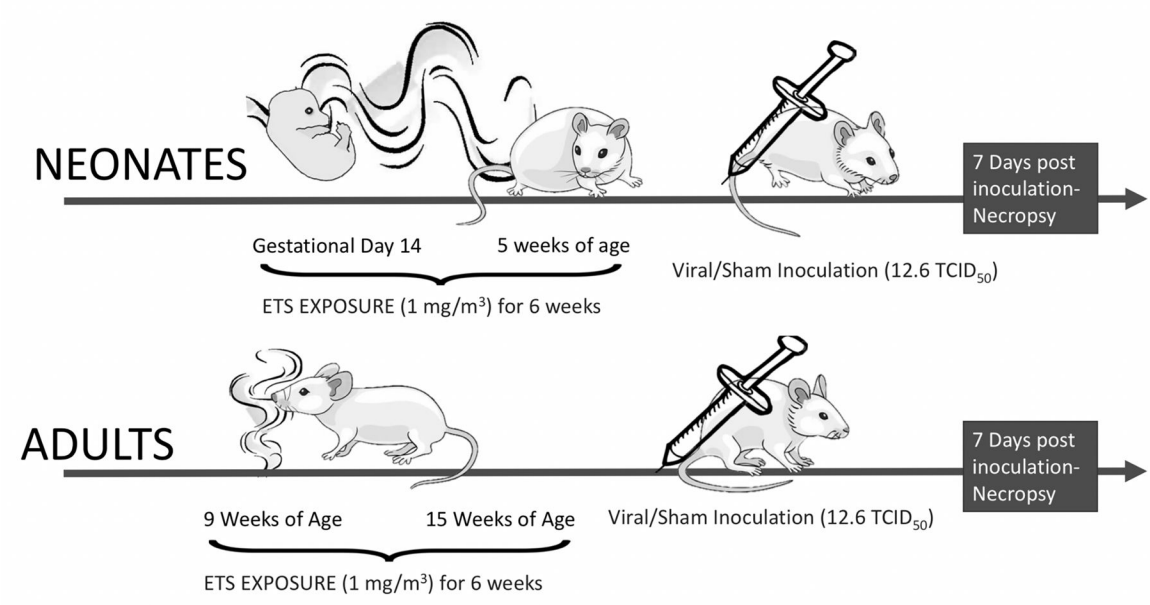

Figure 2. Experimental protocol.

Neonatal BALB/c mice began the 6-week environmental tobacco smoke (ETS) exposure regimen on gestation day 14, or at 9 weeks of age for adults. The mice were exposed to target ETS concentrations of 0 (filtered air control) or 1 mg/m^3 for 6 h/day and 7 days/week, and maintained in a filtered air environment between each 6-hour exposure period. Immediately after the last exposure period, mice were intranasally inoculated with 12.6 $TCID_{50}$ (tissue culture infective dose) Influenza A virus or phosphate-buffered saline (PBS; sham control). Sacrifices occurred 7 days later. n=33–35/group for neonates; n=6/group for adult mice.

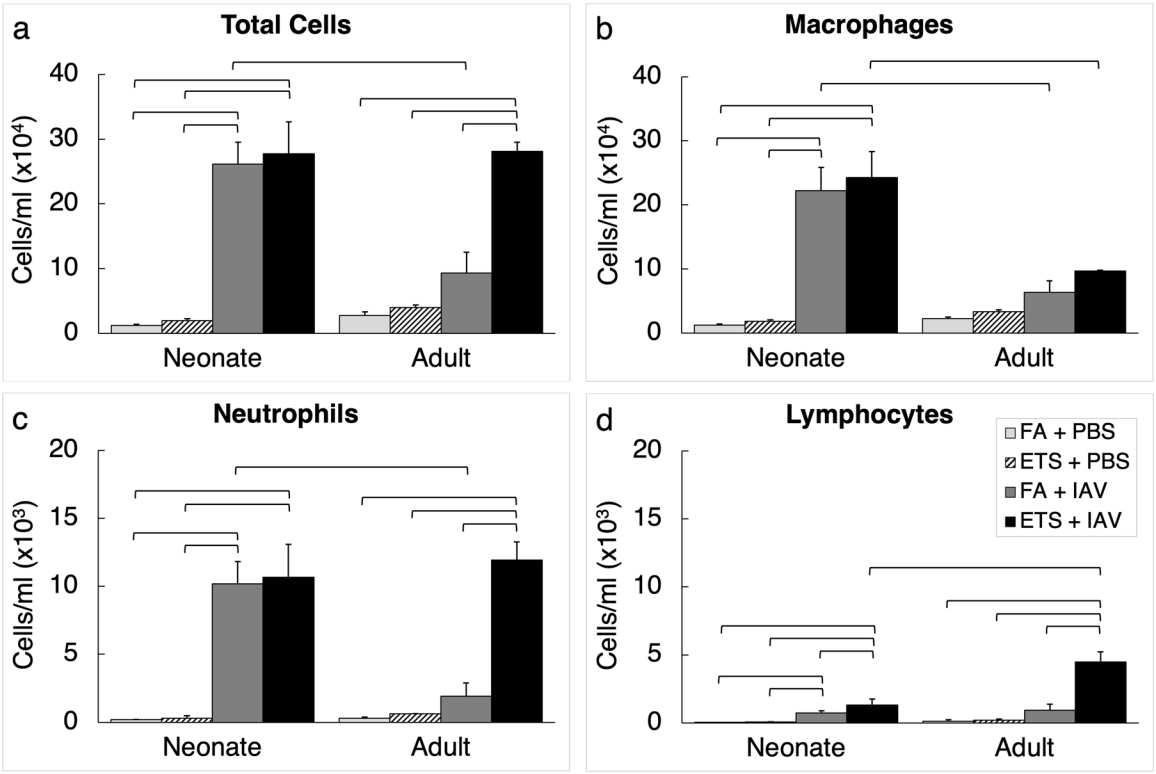

Figure 3. Cell counts from bronchoalveolar lavage fluid (BALF).

Neonatal and adult mice were exposed to filtered air (FA) or environmental tobacco smoke (ETS) for 6 weeks before a single intranasal instillation of phosphate-buffered saline (PBS) or Influenza A virus (IAV). Group data are shown as means ± standard errors of the means (SEMs). There were no statistically significant differences between neonates exposed to ETS+IAV versus FA+IAV. Brackets indicate significant ($p < 0.05$) differences between groups determined by a two-way multivariate ANOVA and Tukey's multiple comparison test. N=33–35/group for neonates or 6/group for adult mice.

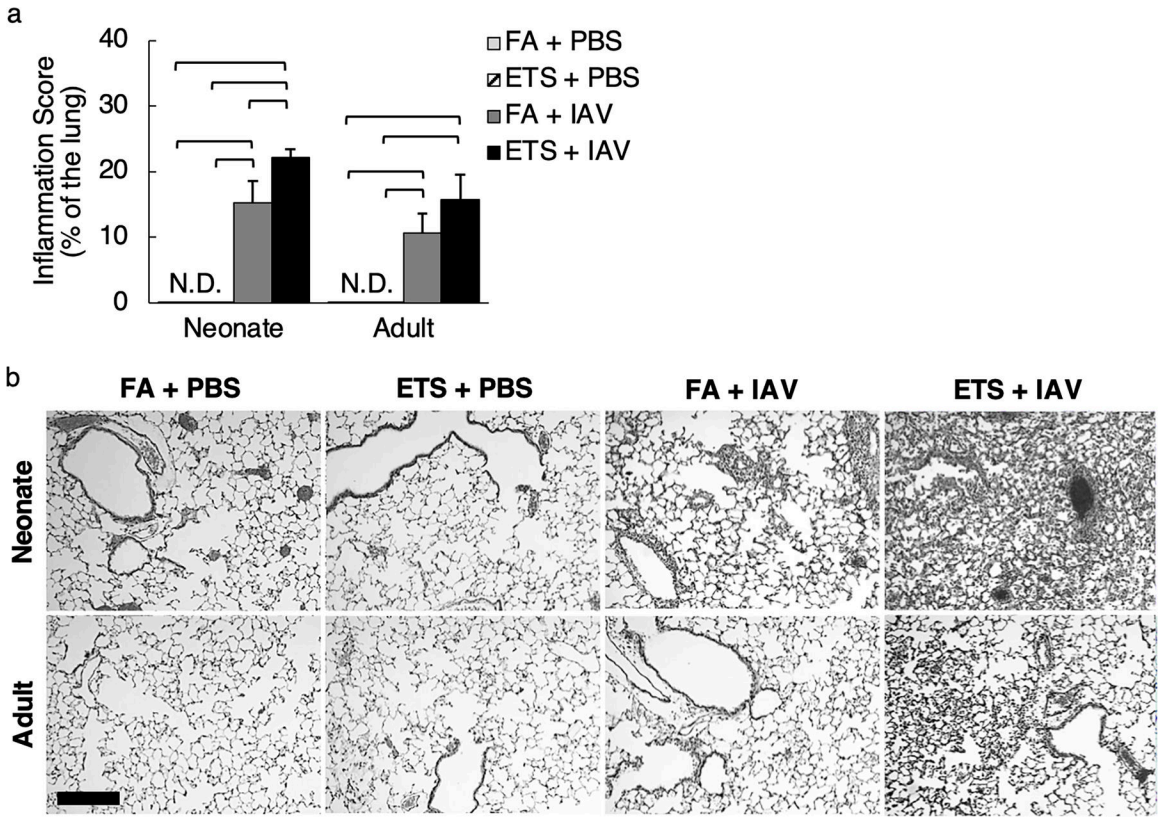

Figure 4. Histopathology of the lung.

The bar graph (panel a) shows the results of semi-quantitative analysis for inflammation in hematoxylin and eosin (H&E)-stained lung tissue sections. Neonatal and adult mice were exposed to filtered air (FA) or environmental tobacco smoke (ETS) followed by inoculation of Influenza A virus (IAV) or phosphate-buffered saline (PBS). All data are expressed as mean ± standard error of the mean (SEM) presented as an inflammation score (% of the whole lung). The limited upper range of the y-axis is due to the lack of an inflammation score (% involved lung parenchyma) that exceeded 40% for any of the groups. N.D. denotes no inflammation was detected. Brackets indicate a significant difference of $p < 0.05$ between groups by 2-way multivariate ANOVA and Tukey's multiple comparisons test. n=10/group for neonates; n=6/group for adult mice. Panel b shows images of H&E-stained lung tissue from neonatal and adult BALB/c mice. The images are representative of the most severe group response. Scale bar is 100 μm.

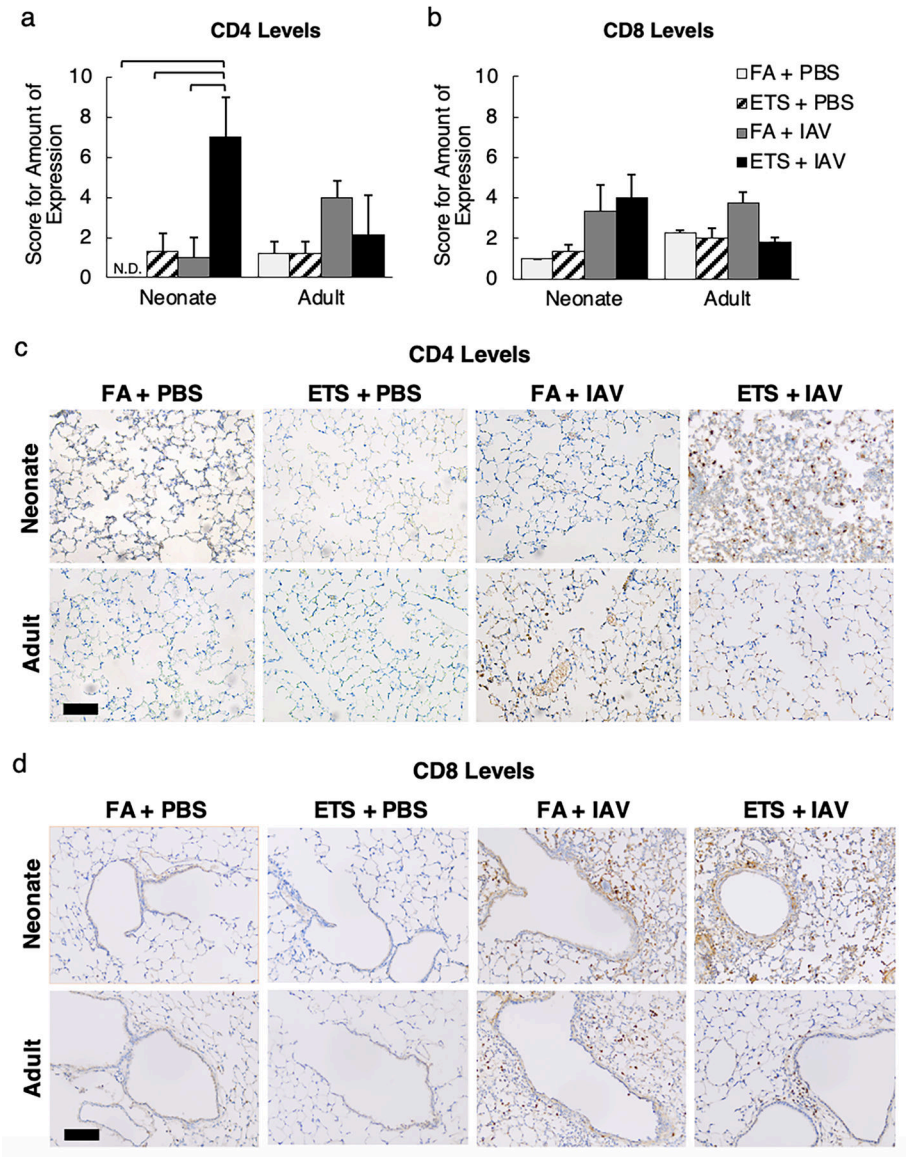

Figure 5. Semi-quantitative analysis of CD4 and CD8 T cell markers in the lungs of mice.

Neonatal and adult mice were exposed to filtered air (FA) or environmental tobacco smoke (ETS) followed by inoculation of Influenza A virus (IAV) or phosphate-buffered saline (PBS). Bar graphs show semi-quantitative assessments of immunohistochemical staining for T cell expression of CD4 (a) and CD8 (b). All data are expressed as mean ± standard error of the mean (SEM). N.D. denotes no staining was detectable. Brackets indicate statistically significant differences between groups ($p < 0.05$; by 2-way multivariate ANOVA and Tukey's multiple comparisons test). n=3/group. Bright-field microscopy images show immunohistochemical staining for CD4 (c) and CD8 (d) proteins in the lungs of neonatal and adult mice. The images are representative of the most severe group response. Scale bars are 100 μm.

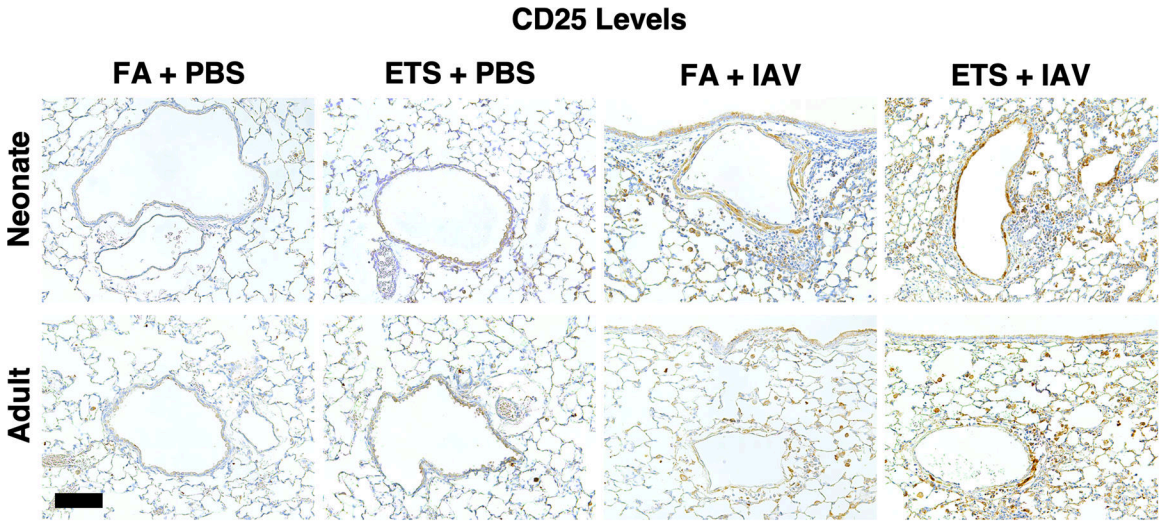

Figure 6. Bright-field microscopy images of immunohistochemical staining for CD25 protein in the lungs of mice.

The images are representative of the most severe group response. Scale bar is 100 μm.

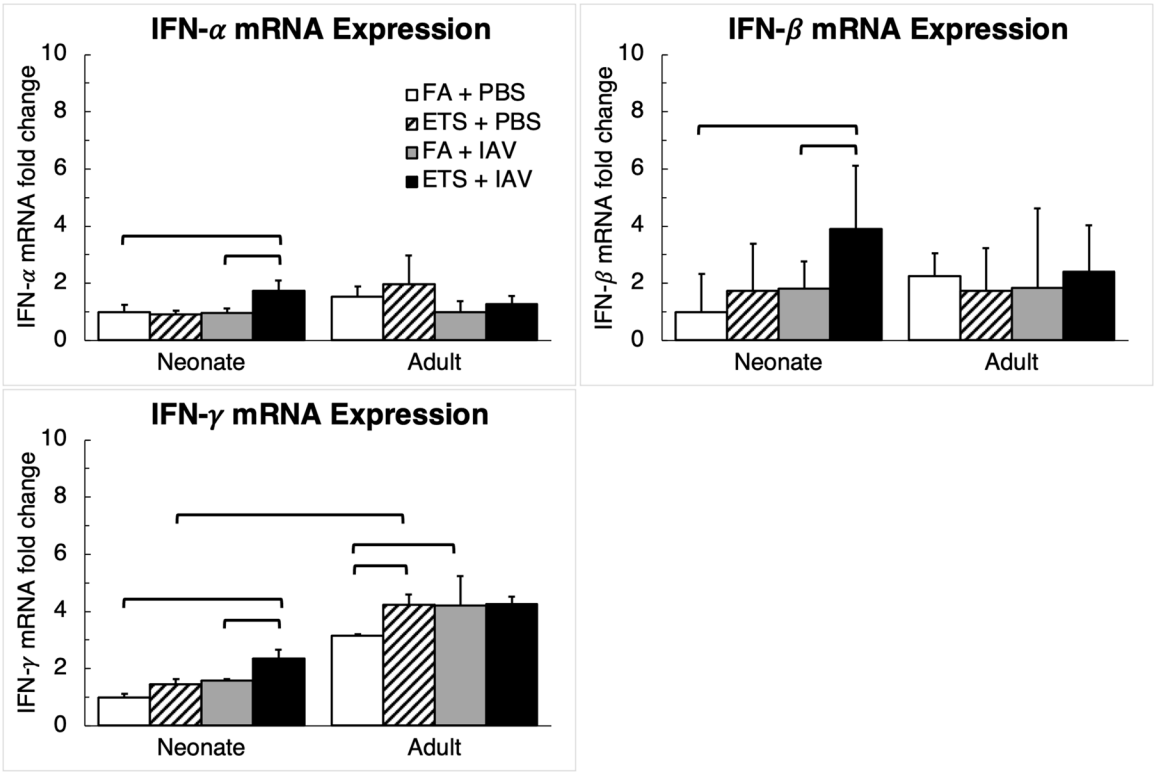

Figure 7. Interferon mRNA expression in the spleen.

Neonatal and adult mice were exposed to filtered air (FA) or environmental tobacco smoke (ETS) followed by inoculation of Influenza A virus (IAV) or phosphate-buffered saline (PBS). Bar graphs show fold change of the expression of interferon (*IFN*)-α, β, and γ mRNA in each group compared to neonatal FA+PBS mice as determined by real-time quantitative reverse transcription-polymerase chain reaction. All data are expressed as the mean ± standard error of the mean. Brackets indicate statistically significant differences between groups ($p < 0.05$; by 2-way multivariate ANOVA and Tukey's multiple comparisons test.) n=9/group for neonates; n=6/group for adult mice.

Table 1.

Semiquantitative scoring rubric for immunohistochemistry

Score	0	1	2	3
Severity	No positive staining	Slightly increased positive staining	Marked increase of positive staining	N/A
Extent	Very little portion of lung section involved	About one quarter of lung section involved	About one half of lung section involved	More than three quarters of lung section involved

Right and/or left lung lobes were examined for each mouse. Total score were calculated for each animal by multiplying severity and extent scores.

Table 2.

Primer sets for gene expression analysis.

Gene	Forward (5’ - 3’)	Reverse (5’ - 3’)
18S	CCATTCGAACGTCTGCCCTAT	GTCACCCGTGGTCACCATG
IFN-α	CTCATAACCTCAGGAACAAGAGAGCCT	GCATCAGACAGGCTTGCAGGTCATT
IFN-β	AAGAGTTACACTGCCTTTGCCATC	CACTGTCTGCTGGTGGAGTTCATC
IFN-γ	CATTGAAAGCCTAGAAAGTCTG	CTCATGAATGCATCCTTTTTCG